crystals

MDPI

Article

Process Design for Continuous Crystallization of L-Tryptophan in Water–Alcohol Solvent Mixtures

Lukas Hohmann, Robert Antpusat (née Hampel) and Norbert Kockmann *

Laboratory of Equipment Design, Department of Chemical and Biochemical Engineering, TU Dortmund University, Emil-Figge-Street 68, 44227 Dortmund, Germany; lukas.hohmann@tu-dortmund.de (L.H.); robert.hampel@tu-dortmund.de (R.A.)

* Correspondence: norbert.kockmann@tu-dortmund.de

Abstract: The study of solid–liquid equilibria in small molecules such as L-tryptophan (L-Trp), which possesses an α-amino group, an α-carboxylic acid group, and an indole compound, presents significant challenges. This research introduces several findings aimed at enhancing process efficiency and sustainability in downstream processing of L-Trp from fermentative origin via crystallization. Transitioning from batch to continuous processes allows for improved scalability and resource management. Furthermore, solubility measurements combined with thermodynamic data from the literature will provide deeper insights into molecular interactions and allow for systematic and data-driven process design. Lab-scale crystallization experiments in both batch and continuous operation allow for the assessment of the process feasibility and solvent impacts on the process and product. The focus is on process development that emphasizes material savings through strategic solvent selection and co-solvent choices.

Keywords: crystallization; solvent choice; solubility improvement; process design

check for updates

Academic Editor: Kannuchamy Vasanth Kumar

Received: 10 March 2025
Revised: 9 April 2025
Accepted: 10 April 2025
Published: 12 April 2025

Citation: Hohmann, L.; Antpusat, R.; Kockmann, N. Process Design for Continuous Crystallization of L-Tryptophan in Water–Alcohol Solvent Mixtures. *Crystals* **2025**, *15*, 355. https://doi.org/10.3390/cryst15040355

Copyright: © 2025 by the authors. Licensee MDPI, Basel, Switzerland. This article is an open access article distributed under the terms and conditions of the Creative Commons Attribution (CC BY) license (https://creativecommons.org/licenses/by/4.0/).

1. Introduction

In the production of high-quality specialty chemicals, which are used in fine chemicals as well as in life science and pharmaceutical products, crystallization is a widely used separation, purification, and preparation method [1]. Products from these industries often have higher molecular weights and higher melting and boiling points compared to low-molecular-weight basic chemicals, as well as an increased thermal sensitivity. These aspects must be considered in process development for achieving an economical and sustainable process performance [2].

In fine and specialty chemistry, batch operation is dominant due to the wide product variety and often low product volumes [3]. A significant disadvantage of batch processes is the potential for variations between individual runs, which can lead to a reduction in product yield and/or quality. Additionally, scaling-up of batch processes often requires adjustments that may compromise product quality or process efficiency. As a result, there is a noticeable trend in both research and industry towards transitioning from batch processes to continuous operations. Continuous processing allows for a high degree of automation and stable operation in steady-state, which helps minimizing quality fluctuations [4]. Furthermore, continuous systems typically require smaller processing equipment compared to batch processes, thereby enhancing the overall process safety [5,6].

In fine chemistry, crystallization is often used as thermal separation process, where a substance is converted from an amorphous (disordered) state into a crystalline, ordered solid [7]. The most commonly used method in industry is the crystallization from a liquid

phase [8], which is applied in industrial sectors such as fine chemicals, life science, and pharmaceuticals production [9,10]. Thus, in the following, crystallization from solutions will be considered. In recent years, the development and improvement of small-scale continuous crystallization processes has gained much relevance, which relates to various factors. One key factor is increasing product quality requirements, often a low amount of product impurities, which must be maintained and ensured for pharmaceutical products. To ensure product quality, variations in the process must be minimized. In addition to purity, other aspects such as crystal shape, size, and morphology play an increasingly important role. These have an influence, for example, on the subsequent further processing in the individual preparation steps of the crystals [11,12].

A gentle method for product recovery and purification is cooling crystallization from solutions [13]. In the literature, many concepts were proposed and characterized ranging from oscillating baffled crystallizer [14] to tank-in-series. To implement and study cooling crystallization in a continuous plug flow operation on the laboratory scale, coiled flow inverter (CFI) devices can be utilized [13,15]. Here, redirected flow counteracts the gravitation [16] and leads to the continuous suspension of the particles and a narrow residence time distribution of both the continuous liquid and the disperse solid phase [17]. The goal of cooling crystallization is often a spherical product with a narrow size distribution for optimal solid–liquid separation (purity) and solids handling [18].

Amino acids are important ingredients in human dietary supplement and animal feeding stuff and are often produced by fermentation. The separation of amino acids from the fermentation broth is laborious and energy-intensive [19]. Tryptophan, in particular L-tryptophan (L-Trp), is an essential amino acid which is industrially produced for use, for example, in food supplements, animal feed, and pharmaceuticals [20]. It can be synthesized in various ways. One important method of production is fermentative production using microorganisms. However, the crude tryptophan obtained in this way, which contains impurities, must be purified before use in food supplements, animal feed, and pharmaceuticals. Known purification processes for crude tryptophan are based on the principle of pH change [21,22]. Like other amino acids, L-Trp is a weak base and is largely protonated in the acidic pH range of the pH change process, as described in [23]. The solubility of the resulting cations of L-Trp in this aqueous solution is significantly increased. In the process of Toshio et al. [21], solid crude tryptophan consisting of solid L-Trp and solid secondary components/impurities, is first dissolved in the aqueous solution of a strong inorganic acid, for example, sulfuric acid, at a low pH of 1 to 4, in particular < 2, close to the saturation concentration. The pH value is then shifted to the neutral range of pH = 5–8 by adding strong inorganic bases, for example, sodium hydroxide solution. Thereby, the isoelectric point, i.e., the pH at which the net charge of the system is zero, is approached, and the solubility of the crystallizing compound is minimized. The isoelectric point of L-Trp in aqueous solution is 5.89 [24]. This supersaturates the solution and the L-Trp crystallizes out as a solid. The solid can be separated from the solution, washed, and dried in further process steps. Although it is described that crystallization takes place in the presence of lower alcohols or ketones, neither a lower alcohol nor a ketone is used in the crystallization step in the examples. This well-known pH change process has numerous disadvantages due to the use of inorganic acids and bases. These have a corrosive effect and require systems and equipment made of high-quality materials. The acids and bases are consumed as auxiliary materials in the process and cannot be easily recovered. The resulting salts must first be removed from the product crystals with the mother liquor during the solid/liquid separation following crystallization, washed with suitable solvents and finally disposed. The accumulation of salts also makes it difficult or impossible to work up and return the mother liquor to the process, leading to a loss of L-Trp. Furthermore, process analysis,

process control and quality assurance are made more difficult by the presence of acids, bases and salts.

The cooling crystallization of L-Trp from water in the presence of gelatin and in the absence of acid, bases, salts and alcohols is described in [25], which enables the generation of so-called spherulitic crystals in a batch process. However, the process is complex, comprises harsh conditions and the gelatin has to be removed again in a further step. The process is based on extremely rapid cooling (quenching) of the solution from 90 °C to 20 °C within a single minute on a laboratory scale, which makes technical implementation and scale-up difficult. Such rapid cooling often prevents high purity in industrial processes.

The aim of this study is to develop a combined process involving continuous evaporation and subsequent cooling crystallization for the recovery of the high-value amino acid L-Trp from raw tryptophan (raw-Trp), which is typically derived from a fermentation process [26]. Various aqueous multi-component solvent systems, consisting of pure water, water and 1-propanol (1-PrOH) or water and iso-propanol (iPrOH), will be investigated for the cooling crystallization. Additionally, an assessment of the cooling crystallization will be conducted to evaluate its suitability and efficiency by comparing it with existing industrial batch process from industry, which often include a pH-shift crystallization with inorganic acids and basis. This comparison will also involve validation through both batch and continuous experiments on the laboratory scale. The results are expected to provide insights into optimizing the recovery process for L-Trp while enhancing efficiency and product quality. The task of the present contribution was therefore to provide an improved process for the purification of L-Trp, which requires fewer steps and/or fewer demands on the apparatus used for this purpose. In particular, a process was to be found which minimizes or completely avoids the use of acids and/or bases.

2. Materials and Methods

2.1. Materials

For all experiments in this work L-Trp (Figure 1, lhs, purity: 99.5%, Evonik AG, Germany) and deionized water is used. 1-propanol (1-PrOH, VWR International, Germany, purity: 100%) and iso-propanol (iPrOH, VWR International, Darmstadt, Germany, purity: 100%) are used as alcohols for the solvent mixtures.



Figure 1. lhs: molecular structure of L-tryptophan including an indole moiety with an amino and carboxyl group. Middle and rhs: experimental setup with jacketed glass vessels for batch crystallization and determining the solubility of L-Trp in water/alcohol solvent mixtures as a function of temperature. Single volume device (lhs) and 4-in-1 device (rhs).

Two temperature-controlled double-jacket glass vessels with a single volume (100 mL) or four individual volumes (65 mL each) (see Figure 1, rhs) are used for batch crystallization

and to determine the solubility, respectively. Both can be tempered using a thermostat (Huber CC 304, Huber, Berching, Germany) or cryostat (Huber Ministat 125, Huber, Berching, Germany). Four magnetic stir bars (PTFE, Crosshead Double, 13 × 17 mm) and one magnetic stirrer plate (MR 1000, Heidolph Instruments & Co. KG, Schwabach, Germany) are used to ensure consistent mixing during solubility experiments.

A lab-scale continuous crystallization setup with CFI cooling crystallizer (d_i = 4 mm, l = 6.54 m, FEP tubing) is used for continuous flow experiments. The basic CFI crystallizer design is described in Hohmann et al. [13] with details on the residence time characterization, while the final setup with storage vessels, pumps, and automation is presented in [27] (see Figure 2).

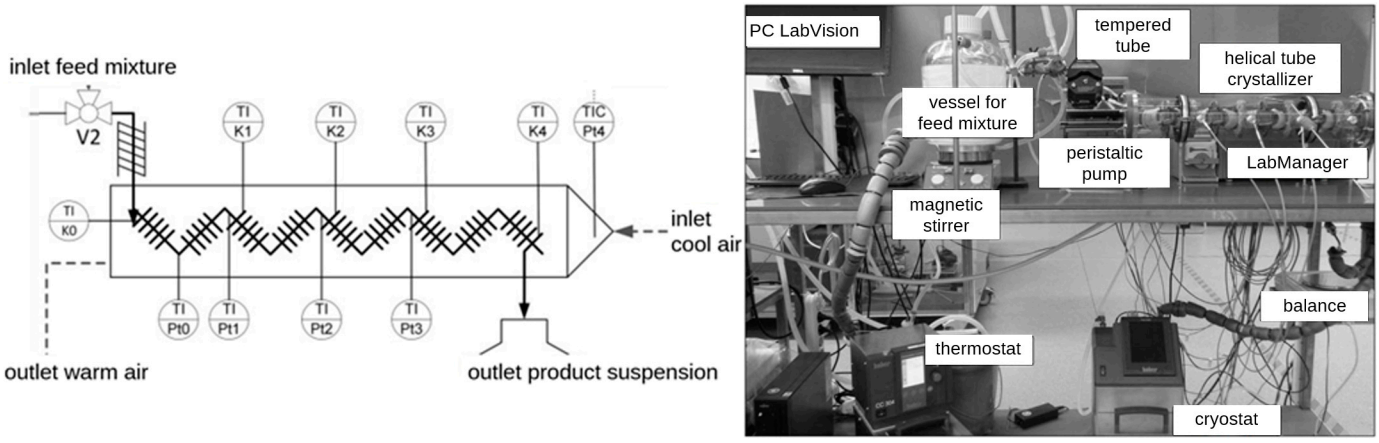


Figure 2. lhs: schematic diagram of the helical tube crystallizer as coiled flow inverter (CFI) [13] with crystallizing solution within a 4 mm tube and counter-current cooling air flow; rhs: experimental setup for carrying out continuous crystallization in the tube crystallizer.

The main device consists of a transparent 4 mm inner diameter and 6.5 m long FEP tube (fluorinated ethylene propylene, wall thickness 1 mm from Bohlender GmbH, Grünsfeld, Germany), which is air cooled in counter-current mode. The FEP tube is helically coiled with mean diameter of 41 mm and 5.5 turns. Nine of these helixes form the CFI with eight 90° bends. More information can be found in [13]. Laboratory scales (Mettler Toledo, MS 300S, ±1 mg and Mettler Toledo, XA 205, ±0.01 mg, Gießen, Germany) are used to determine the masses of the Petri dishes used and the L-Trp samples they contain. To separate the solid content from the solution after equilibration, syringes (10 mL) and syringe filters (cellulose acetate membrane, pore size 0.2 µm) are used. The subsequent drying of the samples is carried out in a desiccator and a vacuum drying oven (Memmert, V0400, Schwabach, Germany). A light microscope (Advance ICD, Bresser GmbH, Rhede, Germany) equipped with a digital camera (Nikon D5300, Nikon, Shinagawa, Japan) is used to analyze samples and crystal habitus after cooling crystallization.

2.2. Solubility Measurement

Solvent systems of pure water, 1-propanol/water (20, 40, and 60 wt.-% 1-PrOH), and isopropanol/water (20, 40, and 60 wt.-% iPrOH) were prepared in glass vessels. In the second step, pure L-Trp was added in excess, the vessel was sealed, and the suspensions were stirred to reach desired temperatures between 10 and 60 °C in intervals of 10 K. The suspensions were stirred at constant temperature for 48 h (equilibrated), resulting in an optically turbid suspension (saturated solution with excess of particles). In detail, the following steps were performed.

The supersaturated suspension is prepared in one of the jacketed glass vessels (see Figure 1). The required amount of L-Trp is added to 40 g of the solvent water in order

to achieve a supersaturated suspension. The MS 300S balance is used for weighing the chemicals. After preparation in a glass vessel, connection to the temperature control unit, and temperature setting, the solution is equilibrated for 48 h while stirring. When determining the solubility of amino acids, times of 24–72 h are often used [23,28–30].

This equilibration duration provides sufficient time to reach a solution concentration close to equilibrium within the accuracy of the analytics process. After 48 h, three suspension samples of approx. 5 g each are taken using a syringe and pressed immediately through a syringe filter (cellulose acetate, pore size 0.2 µm, VWR international, Darmstadt, Germany) and distributed on a Petri dish. The initial sample mass is determined using the MS 300S balance. After complete drying of the sample, the dissolved L-Trp mass is then determined gravimetrically. For this purpose, the Petri dishes with the L-Trp are dried in a drying oven at 60 °C and initially at ambient pressure in order evaporate most of the solvents from the sample. After approx. 4 h, an absolute pressure of 300 mbar abs is set, and the sample is dried further for at least 48 h. The aim is to totally remove the remaining solvent from the sample so that only the previously dissolved equilibrium mass of L-Trp remains the Petri dish after drying. Therefore, the drying conditions and the above mentioned minimum drying duration in the vacuum were carefully validated in the beginning of this study with samples of undersaturated L-Trp solutions of known concentration a mean total error of ±1.7% according to the mass-based L-Trp loading X_{Trp} of the method was found. An incomplete drying of the sample would lead to overestimating the sample concentration or solubility. By subsequently weighing the finally dried sample using the XA 205 balance ($m_{\mathrm{Trp}}{}^{*}$), the solubility of the L-Trp in solvent m_{solv} at the respective equilibration temperature can be determined with the mass ratio $X_{\mathrm{Trp}}{}^{*}$ of the dried material to the solvent mixture mass.

$$X^{*}_{\mathrm{Trp}} = \frac{m^{*}_{\mathrm{Trp}}}{m_{\mathrm{solv}}}$$

This gives a good indication for the quality of the concentration measurements.

2.3. Preparation of Batch Crystallization via Crash Cooling

Preliminary crystallization tests were carried out in test tubes to analyze the resulting crystal habitus and obtain qualitative findings regarding nucleation kinetics as well as the agglomeration tendency of L-Trp in the respective solvent system. The same saturated solution that was prepared and equilibrated for solubility measurements (see Section 2.2) and the same sampling method with syringes equipped with syringe filters (cellulose acetate, pore size 0.2 µm, VWR international, Darmstadt, Germany) were used for these preliminary crystallization tests. Test tubes (10 mL) with screw caps and an ice bath were used for the cooling crystallization. A light microscope (Advance ICD, Bresser GmbH, Rhede, Germany) with camera (Nikon D5300, Nikon, Shinagawa, Japan) was used to analyze the samples after cooling crystallization.

The filtered saturated solution is filled into a test tube. The filtration ensures that no seed crystals are present in the solution. The test tubes were immediately cooled using an ice bath ($T \sim 1$ °C) until a solid formation was observed optically due to turbidity. Placing the relatively slender test tubes in the ice bath causes rapid cooling (so-called crash cooling) of the sample. This procedure corresponds to the procedure for measuring the so-called induction time at the resulting non-critical supersaturation [31,32]. The resulting time interval after the start of crash cooling until the turbidity formation is measured.

A few drops of the resulting suspension are transferred to a Petri dish with a pipette. It was found that the L-Trp crystals adhere directly to the surface of the Petri dish, and the mother liquor can be removed immediately by pouring off. This prevents the crystals

from growing or dissolving during a subsequent optical analysis using a microscope. In addition to the suspensions used to determine the solubility, solutions with a mass fraction of 1-PrOH of 26 wt.-% or 50 wt.-% are prepared at 50 °C, which the same solubility of L-Trp according to the data of Chen et al. [33]. This allows the influence of the alcohol content on the crystal habit and the agglomeration tendency of L-Trp to be investigated at a comparable maximum yield.

2.4. Preparation of Batch Crystallization via Controlled Cooling

In further batch crystallization experiments, three solvent systems were investigated with pure water, water/1-PrOH, and water/iPrOH during controlled cooling at different cooling rates. Thereby, the nucleation dynamics were investigated in terms of the width of the metastable zone (MSZW) [31,32]. Furthermore, the achievable yields and the habitus of the L-Trp crystals were analyzed.

For the experiments, mixed solvents were prepared with $w_{\text{1-PrOH}}$ = 25.6 wt.-% and w_{iPrOH} = 20.0 wt.-%. The amount of L-Trp was dosed according to the measured solubility for the respective solvent composition at 50 °C (see Sections 2.1 and 3.1).

The experiments were performed in the jacketed glass vessel with 100 mL internal volume (see Figure 1, middle image). A glass vial (250 mL) with a screw cap is used as a reservoir to initially prepare 70 g of the L-Trp feed solution in the respective solvent. With the aid of the heated magnetic stirring plate, a magnetic stirring bar and a water bath, the solution was stirred at a temperature of 60 °C for 2 h and dissolved completely, generating a clear solution. A syringe (10 mL) was used to very carefully transfer the solution from the reservoir vial into the preheated jacketed glass vessel in order to prevent crystal formation or depositions closely above the filling level, which might affect the nucleation due to wild seeding in an uncontrolled manner.

During cooling crystallization, the solution was tempered using the cryostat (Huber Ministat 125, Berching, Germany), which was connected to the PC to control it via the LabVision software (vers. 2015, HiTec Zang, Herzogenrath, Germany). The thermostat was connected to a resistance thermometer (Pt100) placed in the solution to ensure control (cascade control) of the solution temperature. The temperature was decreased linearly with various cooling rates from 50 °C to 20 °C, and the formation of the first visible crystals after initial spontaneous nucleation during the batch process was observed with the naked eye and documented via the digital camera and the corresponding temperature was documented, i.e., the limit of the MSZW at the given supersaturation rate [31,32]. The same methods used in Section 2.2 were used for the gravimetric analysis of the resulting mother liquor solution. The crystal habit was again optically analyzed as described in Section 2.3. To determine the maximum or equilibrium yield Y_{Trp}^{*} achievable in a cooling crystallization process, the following equation is used for the temperature range starting from T_0 and ending at T_1 in relation to the solubility at 60 °C of L-Trp.

$$Y_{\text{Trp}}^{*} = \frac{X_{\text{Trp}}^{*}(T_0) - X_{\text{Trp}}^{*}(T_1)}{X_{\text{Trp}}^{*}(T_0)}$$

This value is often called theoretical yield, in comparison to the relative yield Φ_{Trp}, which is the maximum yields Y_{Trp}^{*} relative to the current yield $Y_{\text{Trp}}(t)$ depending on the growth kinetics and dynamics of the crystallization process.

$$\Phi_{\text{Trp}} = \frac{Y_{\text{Trp}}(t)}{Y_{\text{Trp}}^{*}}$$

In these experiments the samples for measuring the yield were drawn after a holding time of 45 min at 20 °C, either after the first appearance of visible crystals (r = 0.5 and 1 K/min experiments), or after the end of the linear temperature ramp (r = 0.1 K/min experiments).

2.5. Preparation of Continuous Crystallization

Continuous crystallization experiments were carried out in the lab scale CFI crystallizer. The solvent mixture of water/iPrOH (w_{iPrOH} = 20.0 wt.-%) is examined exemplarily. In a stirred and temperature-controlled double-jacket vessel of glass for visual observation, 2.5 kg of a 20 wt.-% iPrOH/water mixture was prepared, and an amount of L-Trp was added corresponding to its desired solubility at the desired temperature (see Sections 2.1 and 3.1). A saturated solution at 50 °C is used for experiments 1–5, while a saturated solution at a temperature of 34 °C is used for experiment 6.

The solution was then overheated by 5 K and stirred at this temperature for 2 h to obtain a clear solution. In total, three experimental runs were performed without seeding the incoming solution to induce primary nucleation (experiments 1–3). Optionally, the temperature in the vessel was cooled linearly at a rate of 0.5 K min^{-1} to 2 K below the saturation temperature and held at this temperature for at least 14 h to obtain a crystal suspension via spontaneous nucleation and subsequent equilibration as seed crystal suspension. The desired seed crystal content is 10 wt.-% with respect to the expectable maximum yield at outlet temperature. Three more experimental runs were conducted with seeding (experiments 4–6). The settings for the volume flow rate of air, the temperatures in the thermostat or cryostat and the throughput of the solution for carrying out the experiments using seed crystals are listed in Table 1.

Table 1. Parameter settings for carrying out continuous crystallization using a clear feed solution (1–3) and with seed crystals (4–6).

Experiment -	$\dot{V}_G$ [L min^{-1}]	T (Cryostat) [°C]	T (Thermostat) [°C]	$\dot{m}_L$ [g min^{-1}]	t_L [min]
1/clear feed	10	5	55	5.0 ± 0.2	15.2 ± 0.6
2/clear feed	10	5	55	9.5 ± 0.1	8.2 ± 0.1
3/clear feed	20	5	55	2.5 ± 0.2	31.9 ± 1.6
4/with seed	10	5	48	17.5 ± 0.3	4.4 ± 0.1
5/with seed	10	25	48	17.5 ± 0.2	4.4 ± 0.1
6/with seed	20	20	32	17.5 ± 0.2	4.4 ± 0.1

For preheating and start-up, the CFI cooling crystallizer was fed with deionized water prepared in a second storage tank and heated to the same temperature as a feed storage tank at the desired mass flow rate, while pre-cooled air at the respective volumetric flow rate was introduced counter-currently as the cooling agent.

In total, three experiments were performed without seeding the incoming solution to induce primary nucleation. Samples of the feed suspension were taken when, a steady-state temperature profile was established in the CFI crystallizer and continuous crystallization was started by switching the feed inlet of the CFI crystallizer to the prepared feed storage container via a 3-way valve. The crystallization was observed optically. Samples of the outlet product suspension were analyzed with respect to the remaining solution concentration (yield) and the product crystals were optically analyzed.

3. Results

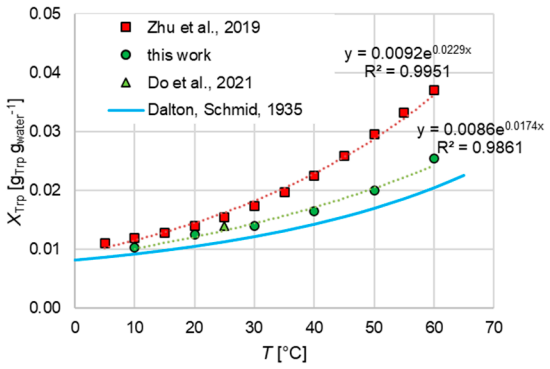
In the previous section, the theoretical and experimental investigations and results are transferred to lab processes to demonstrate the feasibility of the approach.

3.1. Solubility

The measured L-Trp solubility in pure water is compared with data from the literature and modeled with a simple exponential regression analysis, which yields quite good accuracy. The solubility of L-Trp in water increases with increasing temperature. The data are given in Table 2 and show good agreement with the data of Do et al. [34], slightly higher solubility compared to Dalton and Schmidt [35], but lower solubility compared to the work of Zhu et al. [36]. The work of Dalton and Schmidt is from 1933. Since in the original paper, only few details on the experimental methods are provided, slight deviations in solubility might result, e.g., from too short an equilibration time. The higher deviations to the data provided by Zhu et al. are remarkable as they used the same 12 h equilibration time and similar gravimetric analytics as used in this work. These deviations are further discussed in the following based on the mixed-solvent results.

Table 2. Mean values and standard deviations of the determined solubilities of L-Trp in pure water together with graphical display and comparison with the literature values. The diagram compares the experimentally determined solubility data and the literature data according to Dalton and Schmidt [35], Zhu et al. [36], and Do et al. [34]. The standard deviation of the own measurements is indicated with red bars and lies in the range of the symbol size.

T [°C]	X_{Trp}^{*} $[g_{Trp}g_W^{-1}]$	$\sigma(X_{Trp}^{*})$ $[g_{Trp}g_W^{-1}]$	# Equilibrated Suspensions | Total Samples [-]
10	0.01029	$1.17 \cdot 10^{-4}$	2 | 6
20	0.01254	$3.55 \cdot 10^{-4}$	3 | 9
30	0.01406	$3.73 \cdot 10^{-4}$	3 | 9
40	0.01649	$2.11 \cdot 10^{-4}$	3 | 9
50	0.01998	$4.31 \cdot 10^{-4}$	3 | 9
60	0.02547	$8.99 \cdot 10^{-5}$	1 | 3



With adding an alcohol, the solubility increased to a certain concentration and decreases with higher alcohol content. The measurement was performed in alcohol-concentration steps for temperatures ranging from 10 to 60 °C. The experimental results are given in Tables S1 and S2 in the Supporting Information and are graphically shown in Figure 3.

As expected from the pure water results, the solubility in general increases with increasing temperature, both in the 1-PrOH/water- and in the iPrOH/water system. The solubility of L-Trp in the 1-PrOH/water mixture is shown in Figure 3 (lhs) and exhibits a maximum solubility at intermediate solvent composition at roughly 40 wt.-% 1-PrOH in the 1-PrOH/water mixture. This was previously found by Chen et al. [33] and has qualitatively been reproduced in this work. However, solubilities measured by Chen et al. [33] tend to be a little lower compared to the results measured in this work, especially for the lower temperatures range of 20–30 °C. In the higher temperature range, some data points of Chen et al. [33] are in very good agreement with the data measured in this work. The slight deviations in solubility data can be explained by the relatively short equilibration time (20 min) used by Chen et al. [33], compared to this work (48 h) and a more or less step-wise

addition method of Chen et al. [33] compared to sampling and analyzing the equilibrated solution in this work.

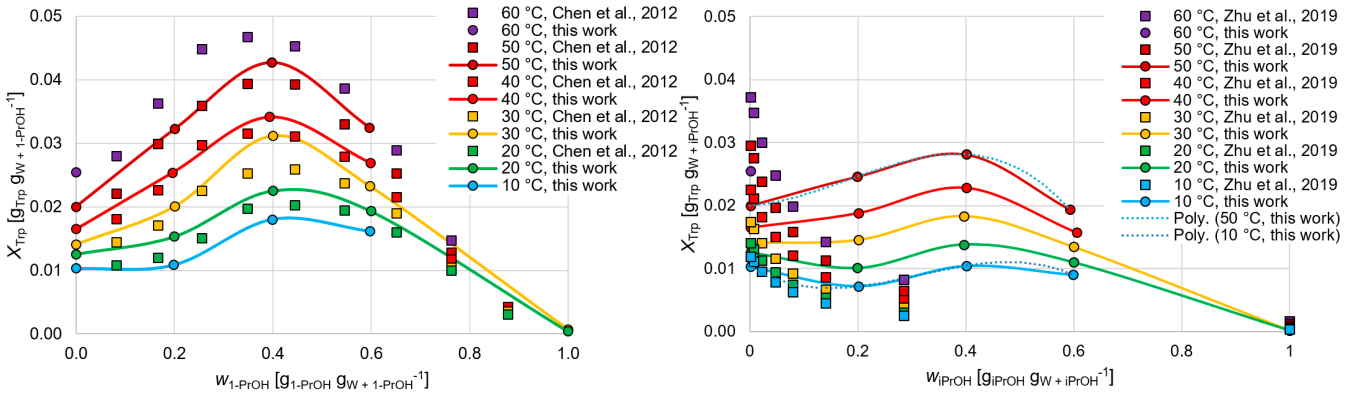


Figure 3. lhs: comparison of the experimentally determined solubility data ("this work" in the legend) and the literature data for the solubilities of L-Trp in water/1-PrOH mixtures according to Chen et al. [33]. Deviations between the data from the present study and the literature data can be attributed to significantly longer isothermal equilibration times in this investigation. rhs: experimentally determined solubility data of L-Trp in water/iPrOH mixtures ("this work" in the legend) with the literature data from Zhu et al. [36] and Do et al. [34]. The lines represent the spline interpolation of data points to guide the readers eye, but no thermodynamic modeling is underlying. The polynomial regression of the measured data was not successful.

In the iPrOH/water mixture, an even more distinctive solubility behavior was found compared to the 1-PrOH/water system results (see Figure 3, rhs). The solubility shows a maximum at roughly 40 wt.-% iPrOH in the iPrOH/water mixture and, in addition, a minimum at roughly 20 wt.-% iPrOH in the iPrOH/water mixture at temperatures of 10–20 °C. The absolute solubility of the iPrOH/water system at respective temperatures is slightly lower compared to the 1-PrOH/water system. Do et al. [34] found comparable minimum/maximum behavior in their measurements at 25 °C. They explained the improved solubility in a certain concentration range with the influence of the indole group within the chemical structure of the amino acid, which improves solute-solvent interactions. The work of Batov et al. [37,38] shows negative enthalpies of solution of L-Trp in water/glycerol mixtures above concentrations of 8 mol-% glycerol in water, indicating a better solubility with increasing alcohol content. Unfortunately, they measured the enthalpies only up to 10 mol-% glycerol in water.

The corresponding data of Zhu et al. [36] for the iPrOH/water system show a completely different trend, in comparison to a typical solvent/antisolvent behavior with water and iPrOH being the solvent and the antisolvent, respectively. A similarly disparate trend has already been discussed by Zhu et al. [36], comparing their solubility data of L-Trp the methanol/water solvent system to the data of Chen et al. [33]. As the data of Chen et al. [33] and Do et al. [34] agree qualitatively very well with this work, showing the same trends in the 1-PrOH/water solvent systems, but the data of Zhu et al. [36] disagree both with Chen et al. [33] (methanol/water solvent system), and with this work (iPrOH/water solvent system), which might be explained by a systematical error in the work of Zhu et al. [36], such as having unknown impurities in their experiments. Hence, their results are excluded in the following investigations.

Samples equilibrated at temperatures >50 °C showed significant yellow discoloration after the equilibration period of 48 h, indicating a chemical change in L-Trp (e.g., decomposition or oxidation) due to thermal stress. To be sure to have the correct crystal morphology, X-Ray powder diffraction (XRPD) measurements were performed at the Laboratory of

Thermodynamics. Crystals from various equilibrated turbid suspensions were analyzed. The results are shown in Figure 4.

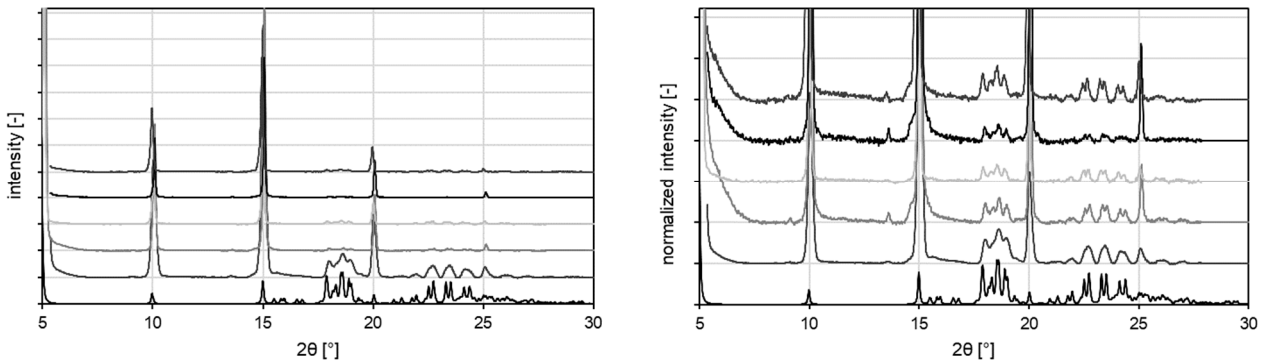


Figure 4. Diffraction patterns from XRPD measurements (lhs: non-normalized; rhs: normalized intensity to the mean of the intensities in the range of 2θ = 17–19° for each individual diffraction pattern) for various samples at 20 °C; from bottom to top: calculated diffraction pattern according to [39] pure L-Trp, L-Trp equilibrated in water, L-Trp equilibrated in 20 wt.-% 1-propanol/water, L-Trp equilibrated in 20 wt.-% isopropanol/water, and L-Trp equilibrated in 40 wt.-% isopropanol/water.

All diffraction patterns of the investigated samples correspond very well with the theoretical pattern of the thermodynamically stable α-polymorph [39], proving that mainly typical hexagonal L-Trp crystals were present in all samples. In the recent literature, two further metastable polymorphs β [40] and α' [41] were isolated and characterized, which seem to have no practical relevance for the systems and process conditions of the present study.

Unfortunately, the regression analysis for the influence of iPrOH and 1-PrOH on the solubility of L-Trp was not successful, since no polynomial, logarithmic, or exponential approach gave sufficient results. Moreover, the complex solubility behavior with maximum (1-PrOH/water systems) or both maximum and minimum (iPrOH/water system) could not be modeled satisfactorily by parameter regression of a standard NRTL model which works well for smaller amino acids in aqueous/alcohol mixed solvent systems [42], showing a classic solvent/antisolvent behavior.

3.2. Batch Crystallization via Crash Cooling

The crash cooling experiments represent a simple and fast experimental method, leading to a first orientation of the kinetical crystallization behavior of unknown systems. However, the crystallization parameters (cooling rate, mixing) are less controlled.

For samples with alcohol in the solvent mixture, an induction time of approx. 10–15 min was measured. In contrast, it takes approx. 30–45 min for crystals to form in samples with only water as a solvent. This behavior can be seen as an initial indication of the different widths of the metastable zone (MSZW), which appears to be narrower for the solvent mixtures than for pure water as the solvent. The MSZW will be described in more detail in the next section.

The desired crystal habit is in general close to a spherical shape due to their good filterability [43]. The temperature influence on the crystal shape was investigated in the range from 30 to 50 °C, but no major influence could be found (see Figure S1 in the Supporting Information). The influence of the alcohol content in the solvent mixture on the crystal shape was already described in the literature, as noted in the introduction. The influence of the two different alcohols on the crystal shape of L-Trp is shown in Figure 5 for pure water and three different alcohol concentrations. Plate-like single crystals were obtained in pure water, while increasing alcohol content in the solvent mixture led to

progressively stacked agglomeration of the single crystals. No compact three-dimensional or needle crystal habitus were observed in pure water.

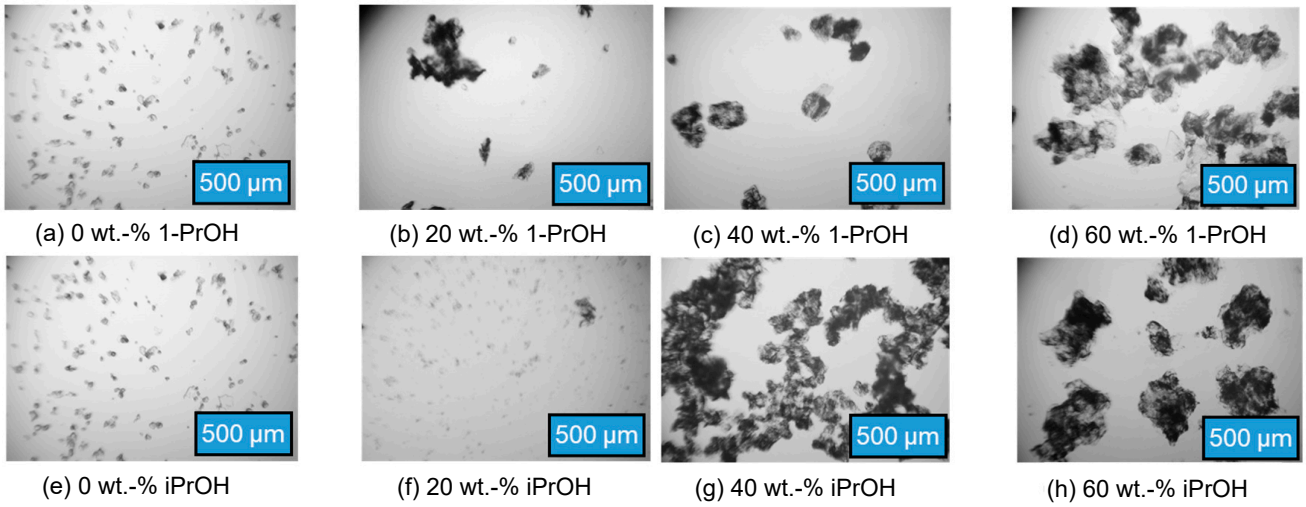


Figure 5. Top row: microscopic images of L-Trp crystals at different 1-PrOH concentrations in the solvent mixture. Crystallization from the saturated solution at 40 °C in an ice bath (~1 °C). Bottom row: microscopic images of L-Trp crystals at different iPrOH concentrations in the solvent mixture. Crystallization from the saturated solution at 40 °C in an ice bath (~1 °C).

The more alcohol is present in the solvent mixture, the more agglomerates are formed, where several platelets form together or overlap. For 1-PrOH, these agglomerates take on a roundish shape (see Figure 5, lhs b-d). There can be two reasons for the increasing agglomerate formation with increasing 1-PrOH content: on the one hand, the increasing proportion of 1-PrOH decreases the surface tension and coalescence of the particles occurs. On the other hand, the higher solubility L-Trp in the saturated solvent mixture leads to higher supersaturation during crash cooling, resulting in the formation of more crystals and thus a higher probability of aggregation and subsequent agglomeration.

Similar results as for 1-PrOH were found for the crystallization and agglomeration in iPrOH/water solvent mixtures (shown in Figure 5, rhs). With 20 wt.-% of iPrOH, only few agglomerates were found. With higher iPrOH content, the agglomerates became more compact. A major difference between the two alcohol/water systems could not be detected, although the maximum solubility of L-Trp in a 40% iPrOH/water mixture at 50 °C is only 2/3 compared to the solubility in a 1-PrOH/water mixture with the same conditions. Hence, agglomerate formation seems to be similar in both alcohol/water systems.

These differences in the crystal shapes are relevant for the further downstream processing, i.e., solid–liquid separation, crystal washing, and drying. The coarse particles from the mixed solvents might be easier to separate compared to the small and thin platelets from the pure water system, but agglomerates are usually prone to mother liquor inclusions which might result in a lower purity. However, the detailed experimental investigation and optimization of the further downstream process steps is not in the focus of this work.

3.3. Batch Crystallization via Controlled Cooling

In the experiments involving controlled cooling within a stirred double-jacket glass vessel, we measured the temperature at which the first visible crystals appeared following spontaneous nucleation (the point at which they could be seen with the naked eye). The results are presented in Figures 6 and 7. In Table S3 in the Supporting Information, the data are given from the experiments.

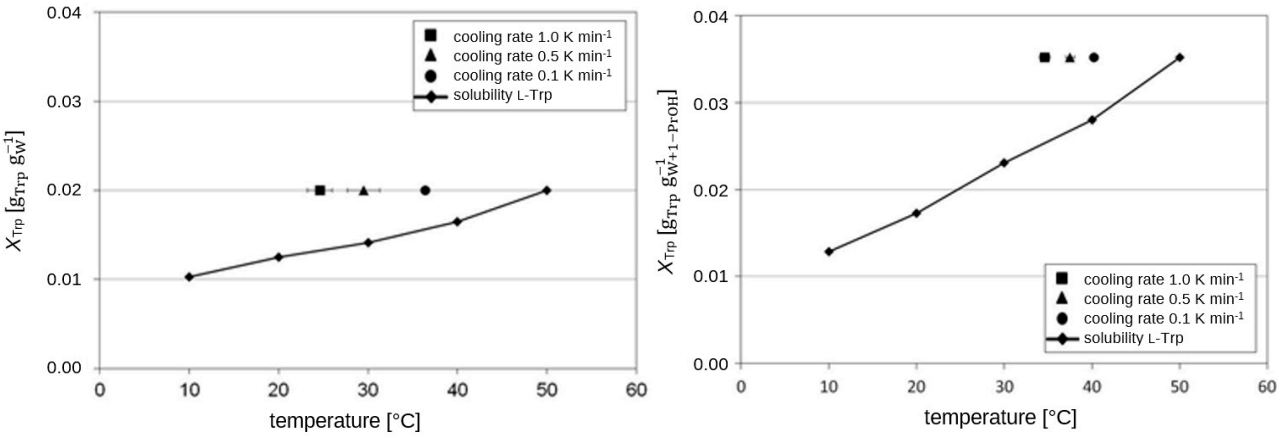


Figure 6. Experimental determination of the metastable range of L-Trp as a function of three different cooling rates in a saturated water solution at 50 °C (lhs) and in the water/1-PrOH solvent system ($w_{1\text{-PrOH}}$ = 25.6 wt.-%) (rhs).

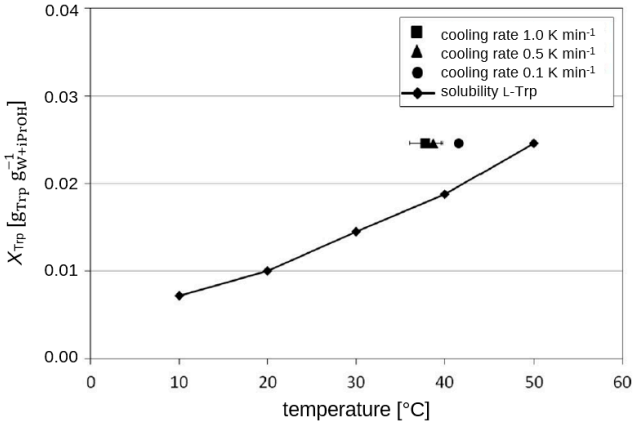


Figure 7. Experimental determination of the metastable range of L-Trp as a function of three different cooling rates in the water/iPrOH solvent system (w_{iPrOH} = 20.0 wt.-%) in a saturated solution at 50 °C.

The MSZW was found be depending on the cooling rates with faster cooling leading to wider MSZW or lower nucleation temperatures, respectively. The iPrOH/water system shows the narrowest MSZW, pure water as a solvent provides the widest MSZW in this comparison.

The optical observation of the first visible crystals after nucleation and the crystallization process revealed an unusual behavior of L-Trp in pure water in perfect accordance with the findings of Kadam et al. [44]. In pure water, individual relatively large primary crystals, so called 'parent crystals', can be observed (see Figure 8, lhs, indicated with red circles). These few crystals exist and grow for a significant period before a secondary nucleation shower can be observed, probably being generated by the attrition of the parent crystals. In the mixed iPrOH/water solvent system, a more classic nucleation behavior was found with numerous primary crystals forming simultaneously. In the following secondary nucleation, attrition, and growth cannot be further differentiated.

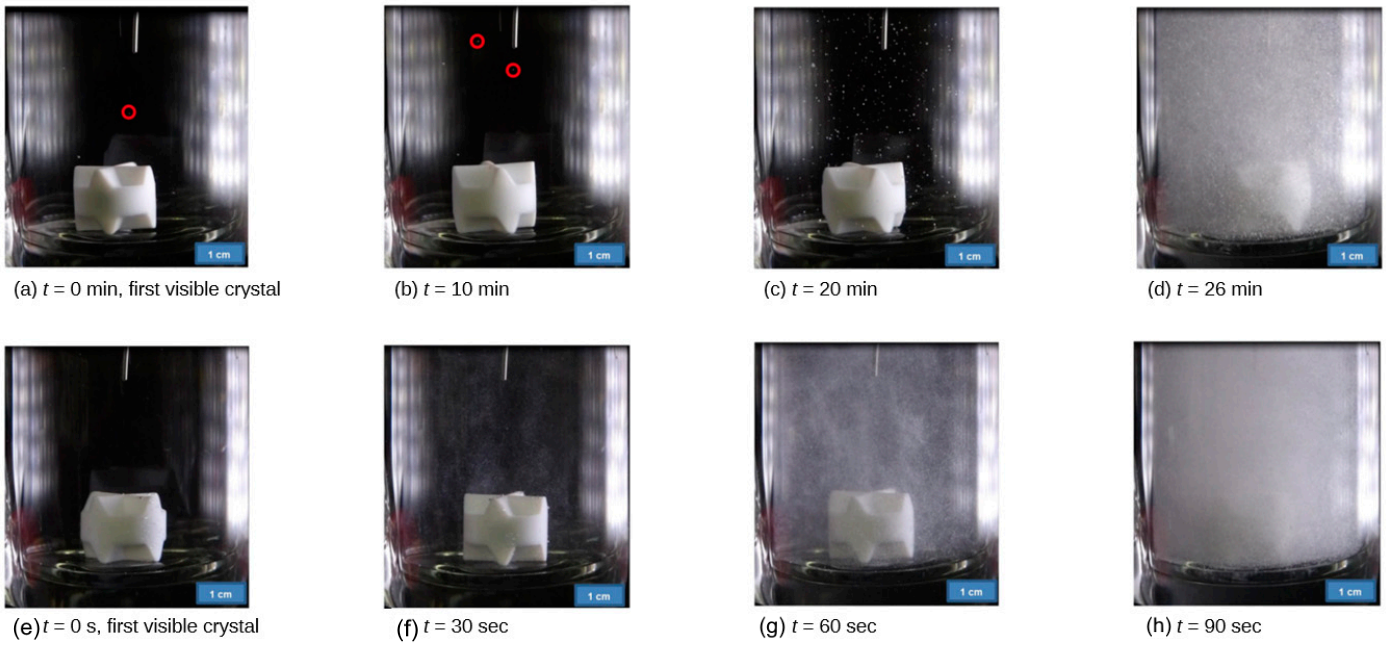


Figure 8. Top row: progression of the crystallization process during batch crystallization of L-Trp in water at r = 1 K min^{-1}. The red circles in the upper two images indicate 'parent crystals' existing for longer duration. Bottom row: progression of the crystallization process during batch crystallization of L-Trp in a water/iPrOH mixture (w_{iPrOH} = 20.0 wt.-%) at r = 1 K min^{-1}. The white descending line is the thermocouple immersed into the solution.

The relative yield is shown in Table 3. It was found that particularly in the PrOH/water system, a yield close to the theoretical yield was achieved, even though the theoretical yield for this system is higher than that in water or in the 1-PrOH/water system. This suggests an unexpectedly high crystal growth rate in this system.

Table 3. Experimentally determined relative yields of the batch tests as a function of the solvent system and the cooling rate r.

Solvent	Y_{Trp}^{*} (50 °C → 20 °C) [%]	Cooling Rate r [K min^{-1}]	Φ_{Trp} [%]
water	37.2	0.1	76.6 ± 5.7
		0.5	75.5 ± 3.8
		1.0	73.5 ± 7.0
water + 1-PrOH $w_{1\text{-PrOH}}$ = 25.6 wt.-%	50.7	0.1	93.4 ± 0.4
		0.5	91.4 ± 1.4
		1.0	92.1 ± 1.9
water + iPrOH w_{iPrOH} = 20.0 wt.-%	59.4	0.1	99.0 ± 0.3
		0.5	97.8 ± 1.1
		1.0	99.5 ± 2.1

Similarly to the findings in Section 3.2, the stacked agglomeration of single crystals was also observed during crystallization from the alcohol/water mixtures, while non-agglomerated single platelet crystals were observed during crystallization from water, as shown in Figure S2 in the Supporting Information. The cooling rate was found not to be very sensitive to the crystal habitus in the investigated range.

3.4. Continuous Crystallization

To exploit the different solubilities of L-Trp in the different alcohol/water systems, continuous processing is beneficial for high yields due to the combination of crystallization and solvent evaporation in successive steps. Hence, continuous crystallization is a major process steps, which will be presented in the following based on the experimental setup described in Section 2.5 with Figure 2. The 20.0 wt.-% iPrOH/water system was chosen, based on the previous results. In addition to the highest possible yield of approx. 59%, which was confirmed experimentally, the solvent system has the narrowest metastable range of ΔT = 12.2 K at a cooling rate of 1.0 K min^{-1} of the three solvent systems investigated in the batch experiments.

Figure 9 (lhs) shows exemplary temperature profiles of the continuous cooling crystallization runs 1 and 3 without seeding. It is noticeable that relatively large temperature differences appear at feed inlet (0 m) and the product outlet (6.54 m) of the crystallizer. In contrast, there is a smaller temperature difference in the middle of the crystallizer. Thus, the axial temperature profile was not perfectly linear, but slightly cubic parabola or s-shaped. A comparable profile was found in run 2. As an overall result from the three experiments without seeding, it was found that the L-Trp in the water/iPrOH solution cannot be continuously operated in the CFI.

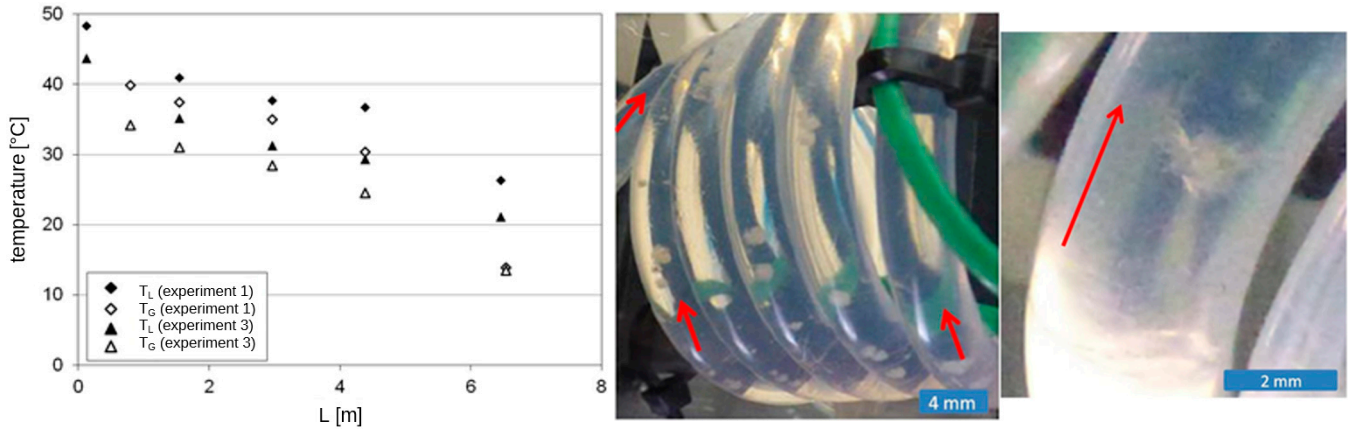


Figure 9. lhs: exemplary temperature profile of the suspension (T_L) and cooling air (T_G) in the CFI crystallizer for experiments 1 and 3. Middle and rhs: nucleation and following growth of L-Trp crystals on the inner tube surface (run 1). Red arrows indicate the direction of flow through the CFI crystallizer coil.

At the low throughput (experimental run 1), primary nucleation occurred on the inner tube surface in the later coil segments 8 and 9 of the CFI crystallizer. The nuclei were stagnant on the wall and grew, resulting in crystallization fouling and complete blockage 20 min after start-up of the run. This experiment was reproduced twice, and the same result was found within 15–20 min after start-up.

At the higher throughput (shorter mean residence time) in experiment 2, no crystals were observable within 60 min inside the CFI crystallizer. Visible crystals appeared in the receiving flask behind at the outlet, even though the solution was widely subcooled with respect to the MSZW found in the batch experiments (see Figure 6). This result agrees well with previous findings of our group with the L-alanine/water system in the same CFI crystallizer setup [13]. The significantly increased cooling rate (r ≈ 3 K/min) compared to the batch processes, combined with the extremely smooth surface of the fluorinated ethylene propylene (FEP) tubing of the crystallizer, the absence of a gas–liquid interface and the well-defined laminar flow regime result in enlarged MSZW, allowing for significantly higher supersaturations compared to batch. In experiment 3, the same behavior as that in

experiment 1 was found, but the nucleation and growth of crystals on the tube wall was shifted to segments 3–4. Again, the blockage of the tube occurred after 20 min.

The decision to start with a saturated, seeded solution was clear after the experience with the unstable operation with primary nucleation. In experiment 4, an inlet temperature of 50 °C was applied. The growth of seed crystals was observed during continuous crystallization optically by the increasing turbidity along the crystallizer length. The suspension flow was homogenous and without crystal settling in the entire crystallizer (see Figure 10).

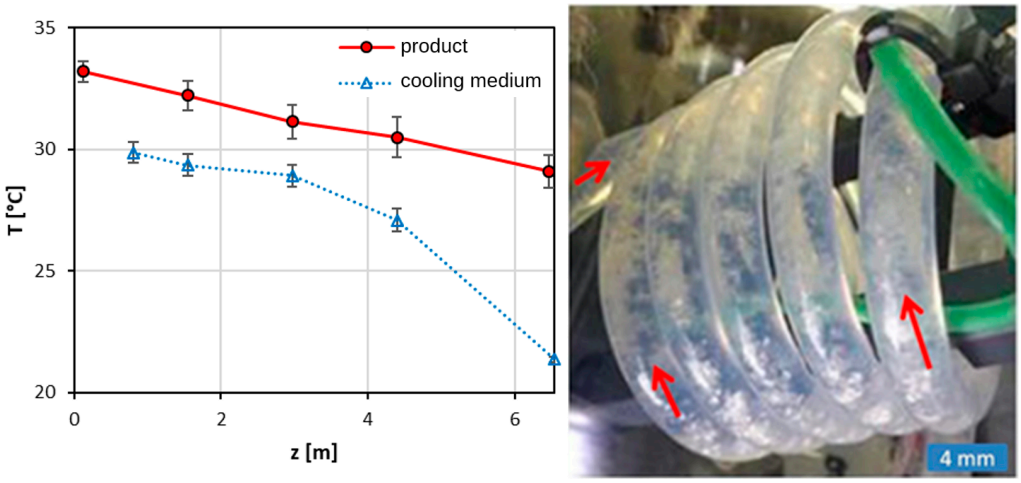


Figure 10. lhs: typical axial temperature profile of the product T_L and cooling medium T_G during the continuous cooling crystallization of L-Trp in the coiled tube cooling crystallizer. rhs: crystal flow in the direction of the red arrow and growth during experiment 4 in the lower area of segment 9 of the tube crystallizer indicating good suspension also in the lower tube part.

After an operation time of approx. 10 min, crystal adhesion occurred also in segments 8 and 9, as well as in the outlet drain, which caused blocking of the crystallizer within a further 10 min. To counteract this, the cryostat for the cooling air was set to a temperature of 25 °C in experiment 5 resulting in a gas inlet temperature of approx. 25.8 °C, resulting in a temperature difference of >10 K between crystal suspension and cooling agent at the outlet of the tube crystallizer, which again led to crystal adhesions and fouling. After approximately 5 min after the first adhesions formed in the outlet, the adhesions also spread to segments 8 and 9 until blockages occurred after a total of 30 min and the experiment had to be stopped. This behavior was reproduced three times in an identical manner.

As a result of the preliminary continuous experiments, the entire temperature profile in experiment 6 was shifted to lower temperatures, including the temperature in the feed vessel. The temperature difference in the outlet between the solution and the cooling air was adjusted to a range of approx. 5–6 K to prevent adhesions.

With these optimized settings an average cooling rate of 1.13 K min^{-1} was obtained. It was possible to operate the CFI crystallizer stably, consuming the entire feed vessel content with a total mass of approx. 3 kg through the tubular crystallizer over a period of approx. 2.5 h without facing critical adhesion leading to blockages. Only small deposits occurred in segments 8 and 9 in the lower area of the horizontal tube coils after approx. 1.5 h, but these did not affect the robust operation of the crystallizer. As these sedimentations were only observed in the gravity-facing area of the tube, they can be explained by settling of large product crystals.

The installed operation conditions for the experiment 6 with seed suspension as a feed material. Through a thermogravimetric analysis of both the seed crystal solution and product solution (mother liquor), the relative yield of the continuous crystallization

process in experiment 6 based on the solubility data at the exit temperature of 29.1 °C was determined to be Φ_{Trp} = 36.3%. This relatively low yield compared to the batch results, see Table 3 can be explained by the relatively low mean residence time of t_L= 4.4 min in this lab-scale CFI crystallizer at the given flow rate, see Table 1 and the significantly smaller $\Delta T_{in,out}$ = 4.9 K compared to 30 K in the corresponding batch experiments (45 min annealing time; see Section 2.5). From the quasi-linear temperature profile (see Figure 10) and the mean residence time, a cooling rate of r_{CFI} = 1.1 K min^{-1} can be calculated, which also exceeds the investigated cooling rates in the batch mode. In a technical continuous process crystallization process of L-Trp, a crystallizer with a higher mean residence time at a given throughput and ΔT would be required.

3.5. Design of Continuous Downstream Process

The presented findings on solubility and crystallization characteristics of L-Trp were utilized to propose a process for continuous downstream processing and purification of L-Trp from raw tryptophan (raw-Trp), in particular by raw-Trp obtained by fermentation and the concentration of the fermentation broth [45]. The suggested process is depicted in Figure 11 and comprises the following steps:

(1) Dissolving raw-Trp in a solvent system that includes water and alcohols at a temperature of up to 50 °C to avoid thermal decomposition of L-Trp: A saturated solution should be obtained, e.g., by a CSTR-type setup with a clear solution withdrawal.
(2) Optionally concentrating the solution obtained in step (1) at a temperature of up to 50 °C: This concentration step could be either realized by evaporation/distillation under reduced pressure or the use of suitable membranes.
(3) Performing cooling crystallization of the L-Trp from the solution to a temperature below 20 °C: The optional dosing of seed crystals (either dry or dispersed in liquid) depends on the actual crystallizer setup, but is recommended based on the presented experimental results to achieve a robust and reproduceable process; and
(4) Separating the solid L-Trp in crystalline form from the liquid phase, e.g., by filtration, sedimentation or centrifugation: After mechanical separation of the crystals, further purification, e.g., by crystal washing or drying can be conducted.

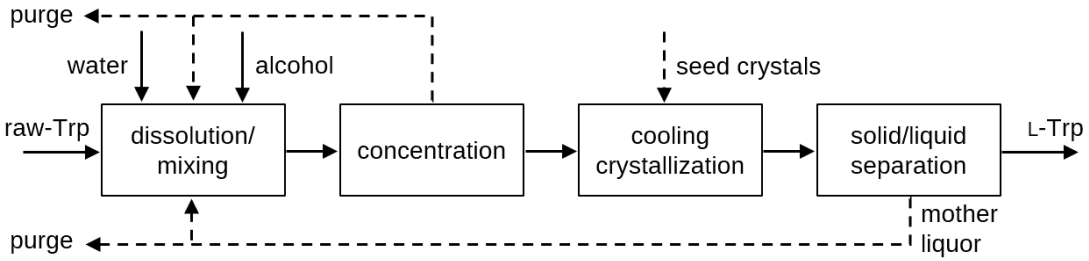


Figure 11. Proposed L-Trp downstream process with concentration step; the dotted lines indicate optional steps.

In principle, such a purification process can be conducted either continuously or as a batch process. However, in a continuous process, the mother liquor of the mechanical separation step (4) can be recycled directly to maximize the overall yield of the process. The recycling of mother liquor could be limited by an accumulation of impurities from the fermentation, which must be determined for the individual sources of the raw-Trp. The detection of the impurities depends on the upstream process and cannot be discussed here in detail. Thus, a purge of mother liquor might be necessary, depending on the concentration of individual impurities in the raw-Trp and their impact, e.g., on the crystallization process and purity of the crystals. However, the separated stream in the concentration step (2) and

withdrawal of mother liquor in the residual moisture of the mechanically separated L-Trp product crystals in step (4) represent a potential outlet for impurities.

The recyclability of the mother liquor in such a continuous cooling crystallization-based purification process of L-Trp is a major measure to overcomes the typical disadvantages of classic batch pH-shift crystallization-based processes as described in the introduction.

Regarding the solvent selection, the iPrOH/water system appears to be the most advantageous. Additionally to the highest possible yield of approx. 59%, the solvent system has the narrowest metastable range of ΔT = 12.2 K at a cooling rate of 1.0 K min^{-1} of the three solvent systems investigated in the batch experiments. The unusual solubility behavior of the iPrOH/water system could be utilized to maximize the yield even more and minimize the solvent consumption. To do so, the dissolution step (1) of raw-Trp could be performed at w_{iPrOH} = 40% (maximum solubility), whereas in the concentration step, the solvent composition could be adjusted to $w_{\text{iPrOH}} \approx$ 20% (minimum solubility at lower temperatures) to maximize the yield in the crystallization. Alternatively, the iPrOH/water system could be operated without the concentration and solvent composition shifting step (2), resulting in a lean production process. To minimize the solvent consumption, a composition of $w_{\text{1-PrOH}}$ = 40% (maximum solubility) would be beneficial as well.

4. Conclusions

The crystallization of small molecules from aqueous solutions is often assisted by additives to control solubility and crystal shape and agglomeration behavior. This contribution describes the solubility and cooling crystallization characteristics of L-Tryptophan (L-Trp) from 1-propanol (1-PrOH)/water and iso-propanol (iPrOH)/water solvent mixtures in the temperature range from 60 °C to 20 °C. By adding the alcohols, the solubility can be drastically increased by more than 100% compared to the solubility in pure water. The crystallization process was investigated in batch and in continuous operation with different weight percentages of alcohol in the mixed solvent system. While the concentration and type of alcohol have a major influence on the solubility and agglomeration of the otherwise thin platelet-like crystals, the temperature had a major influence on the solubility of L-Trp in the solvent mixtures. A continuous crystallization process was investigated on lab-scale in a coiled flow inverter (CFI) cooling crystallizer without internals and could be successfully operated in steady-state without blockages for several hours with a seeding strategy. This can serve as a base for a completed continuous purification process consisting of a tubular plug flow crystallizer in combination with an evaporator for solvent concentration, continuous seeding as well as solid–liquid separation and mother liquor recycle for improved yield. Although the focus of the presented results was on rapid process development in early stage, the emphasizes material savings through strategic solvent selection and co-solvent choices can be used for current production processes.

Supplementary Materials: The following supporting information can be downloaded at: https://www.mdpi.com/article/10.3390/cryst15040355/s1, Figure S1: lhs: Microscope images of the L-Trp crystals formed at different 1-PrOH-proportions in the solvent of the saturated solution at 30 °C after crystallization in an ice bath; rhs: Microscope images of the L-Trp crystals formed at different iPrOH proportions in the solvent of the saturated solution at 50 °C after crystallization in an ice bath.; Figure S2: top row: Product crystals from batch cooling crystallization at a cooling rate of 0.5 K min^{-1} from various solvent systems. Bottom row: Product crystals from batch cooling crystallization at a cooling rate of 1.0 K min^{-1} from various solvent systems.; Table S1: Results and standard deviations of the determined solubilities of L-Trp in water/1-PrOH mixtures; Table S2: Results and standard deviations of the determined solubilities of L-Trp in water-iPrOH mixtures; Table S3: Widths of the MSZW as a function of the solvent system and the cooling rate r.

Author Contributions: Conceptualization: L.H. and N.K.; methodology: L.H.; software: L.H. and R.A.; validation: L.H. and N.K.; formal analysis: L.H. and N.K.; investigation: L.H. and R.A.; resources: N.K.; data curation: L.H. and R.A.; writing—original draft preparation: N.K.; writing—review and editing: L.H., R.A. and N.K.; visualization: L.H., R.A. and N.K.; supervision: L.H. and N.K.; project administration: N.K.; funding acquisition: N.K. All authors have read and agreed to the published version of the manuscript.

Funding: This research was funded by the Federal Ministry for Economic Affairs and Climate Action (BMWK) as part of the ENPRO SMekT project (grant number 03ET1254D).

Data Availability Statement: The original contributions presented in the study are included in the article/Supplementary Material. Further inquiries can be directed to the corresponding author/s. The Supplementary Material is provided for this article and contains further detailed information regarding the experimental data.

Acknowledgments: The authors thank Carsten Schrömges (TU Dortmund University, BCI Laboratory of Equipment Design) for his technical support, Christoph Held (TU Dortmund University, BCI Laboratory of Thermodynamics) for the conceptual and methodical support for the solubility experiments and discussion on the results, and Christian Lübbert (TU Dortmund University, BCI Laboratory of Thermodynamics) for XRPD measurements.

Conflicts of Interest: On behalf of all authors, the corresponding authors state that there is no conflict of interest.

Abbreviations

The following abbreviations are used in this manuscript.

1-PrOH	1-propanol
CFI	Coiled flow inverter
ENPRO	Energieeffizienz und Prozessbeschleunigung—Energy efficiency and process acceleration
iPrOH	Iso-propanol or 2-propanol
lhs	Left-hand side
L-Trp	L-tryptophan
MSZW	Metastable zone width
Raw-Trp	Raw tryptophan
rhs	Right-hand side
SMekT	Smart miniplants for efficient continuous separation processes
XRPD	X-ray powder diffraction

References

1. Mersmann, A.; Kind, M.; Stichlmair, J. *Thermische Verfahrenstechnik: Grundlagen und Methoden*; Springer: Berlin, Germany, 2005.
2. Adjiman, C.S.; Sahinidis, N.V.; Vlachos, D.G.; Bakshi, B.; Maravelias, C.T.; Georgakis, C. Process systems engineering perspective on the design of materials and molecules. *Ind. Eng. Chem. Res.* **2021**, *60*, 5194–5206. [CrossRef]
3. Pollak, P. *Fine Chemicals: The Industry and Business*; Wiley: Hoboken, NJ, USA, 2011.
4. Grundemann, L.; Schoenitz, M.; Scholl, S. Shorter Time-to-Market with Micro-Conti Processes. *Chem. Ing. Tech.* **2012**, *84*, 685–693. [CrossRef]
5. Holtze, C.; Boehling, R. Batch or flow chemistry?—A current industrial opinion on process selection. *Curr. Opin. Chem. Eng.* **2022**, *36*, 100798. [CrossRef]
6. Kockmann, N.; Thenée, P.; Fleischer-Trebes, C.; Laudadio, G.; Noël, T. Safety assessment in development and operation of modular continuous-flow processes. *React. Chem. Eng.* **2017**, *2*, 258–280. [CrossRef]
7. Beckmann, W. Introduction. In *Crystallization*; Beckmann, W., Ed.; Wiley-VCH: Weinheim, Germany, 2013.
8. Beckmann, W. Grundlagen der Kristallisation. In *Kristallisation in der Industriellen Praxis*; Hofmann, G., Ed.; Wiley-VCH: Weinheim, Germany, 2004.
9. Roberge, D.M.; Ducry, L.; Bieler, N.; Cretton, P.; Zimmermann, B. Microreactor Technology: A Revolution for the Fine Chemical and Pharmaceutical Industries? *Chem. Eng. Technol.* **2005**, *28*, 318–323. [CrossRef]

10. Kirwan, D.J.; Orella, J. Crystallization in the Pharmaceutical and Bioprocessing Industries. In *Handbook of Industrial Crystallization*, 2nd ed.; Myerson, A.S., Ed.; Butterworth-Heinemann: Woburn, UK, 2001.
11. Tung, H.-H.; Paul, E.L.; Midler, M.; McCauley, J.A. *Crystallization of Organic Compounds: An Industrial Perspective*; John Wiley & Sons Inc.: Hoboken, NJ, USA, 2009. [CrossRef]
12. Wong, S.Y.; Tatsuoko, A.P.; Trout, B.L.; Myerson, A.S. Development of Continuous Crystallization Processes Using a Single-Stage Mixed-Suspension, Mixed-Product Removal Crystallizer with Recycle. *Cryst. Growth Des.* **2012**, *12*, 5701–5707. [CrossRef]
13. Hohmann, L.; Gorny, R.; Klaas, O.; Ahlert, J.; Wohlgemuth, K.; Kockmann, N. Design of a Continuous Tubular Cooling Crystallizer for Process Development on Lab-Scale. *Chem. Eng. Technol.* **2016**, *39*, 1268–1280. [CrossRef]
14. Lawton, S.; Steele, G.; Shering, P. Continuous Crystallization of Pharmaceuticals Using a Continuous Oscillatory Baffled Crystallizer. *Org. Process Res. Dev.* **2009**, *13*, 1357–1363. [CrossRef]
15. Schmalenberg, M.; Kreis, S.; Weick, L.K.; Haas, C.; Sallamon, F.; Kockmann, N. Continuous Cooling Crystallization in a Coiled Flow Inverter Crystallizer Technology—Design, Characterization, and Hurdles. *Processes* **2021**, *9*, 1537. [CrossRef]
16. Saxena, A.K.; Nigam, K.D.P. Coiled configuration for flow inversion and its effect on residence time distribution. *AIChE J.* **1984**, *30*, 363–368. [CrossRef]
17. Hohmann, L.; Schmalenberg, M.; Prasanna, M.; Matuschek, M.; Kockmann, N. Suspension Flow Behavior and Particle Residence Time Distribution in Helical Tube Devices. *Chem. Eng. J.* **2019**, *360*, 1371–1389. [CrossRef]
18. Liu, Y.; Ma, Y.; Yu, C.; Gao, Y.; Li, K.; Tong, L.; Chen, M.; Gong, J. Spherical agglomeration of high melting point drugs in water at low temperature by developing a two-step oiling-out mechanism and the design strategy. *Green Chem.* **2022**, *24*, 5779–5791. [CrossRef]
19. Mandal, S.; Kulkarni, B.D. Separation strategies for processing of dilute liquid streams. *Int. J. Chem. Eng.* **2011**, *1*, 659012. [CrossRef]
20. Yokota, A.; Ikeda, M. (Eds.) *Amino Acid Fermentation*; Springer: Berlin/Heidelberg, Germany, 2017; ISBN 978-4-431-56520-8.
21. *EP 0 274 728 A1*; Method for Purifying Tryptophan. EPO: Munich, Germany, 1988.
22. *US 6 284 897*; Method for Crystsalizing Tryptophan. Ajinomoto Co. Inc.: Tokyo, Japan, 2001.
23. Needham, T.E.; Paruta, A.N.; Gerraughty, R.J. Solubility of Amino Acids in Pure Solvent Systems. *J. Pharm. Sci.* **1971**, *60*, 565–567. [CrossRef] [PubMed]
24. Dey, B.P.; Dutta, S.; Lahiri, S.C. Dissociation Constants of Amino Acids in Isopropanol +Water Mixtures. *Indian J. Chem.* **1992**, *21*, 886.
25. Yang, J.; Wang, Y.; Hao, H.; Xie, C.; Bao, Y.; Yin, Q.; Gong, J.; Jiang, C.; Hou, B.; Wang, Z. Spherulitic crystallization of L-tryptophan: Characterization, growth kinetics, and mechanism. *Cryst. Growth Des.* **2015**, *15*, 5124–5132. [CrossRef]
26. Leuchtenberger, W.; Huthmacher, K.; Drauz, K. Biotechnological production of amino acids and derivatives: Current status and prospects. *Appl. Microbiol. Biotechnol.* **2005**, *69*, 1. [CrossRef]
27. Hohmann, L.; Greinert, T.; Mierka, O.; Turek, S.; Schembecker, G.; Bayraktar, E.; Wohlgemuth, K.; Kockmann, N. Analysis of Crystal Size Dispersion Effects in a Continuous Coiled Tubular Crystallizer: Experiments and Modelling. *Cryst. Growth Des.* **2018**, *18*, 1459–1473. [CrossRef]
28. Wohlgemuth, K. Induced Nucleation Processes During Batch Cooling Crystallization. Ph.D. Thesis, TU Dortmund University, Dortmund, Germany, 2012.
29. Orella, C.; Kirwan, D. The Solubility of Amino Acids in Mixtures of Water and Aliphatic Alcohols. *Biotechnol. Prog.* **1989**, *5*, 89–91. [CrossRef]
30. Held, C.; Reschke, T.; Müller, R.; Kunz, W.; Sadowski, G. Measuring and modeling aqueous electrolyte/amino-acid solutions with ePC-SAFT. *J. Chem. Thermodyn.* **2014**, *68*, 1–12. [CrossRef]
31. Beckmann, W. Mechanisms of Crystallization. In *Crystallization*; Beckmann, W., Ed.; Wiley-VCH: Weinheim, Germany, 2013.
32. Garcıa-Ruiz, J.M. Nucleation of protein crystals. *J. Struct. Biol.* **2003**, *142*, 22–31. [CrossRef] [PubMed]
33. Chen, Q.; Wang, J.; Bao, Y. Determination of the crystallization thermodynamics and kinetics of l-tryptophan in alcohols–water system. *Fluid Phase Equilib.* **2012**, *313*, 182–189. [CrossRef]
34. Do, H.T.; Franke, P.; Volpert, S.; Klinksiek, M.; Thome, M.; Held, C. Measurement and modelling solubility of amino acids and peptides in aqueous 2-propanol solutions. *Phys. Chem. Chem. Phys.* **2021**, *23*, 10852–10863. [CrossRef]
35. Dalton, J.B.; Schmidt, C.L.A. The Solubilities of Certain Amino Acids and Related Compounds in Water, the Densities of their Solutions at Twenty-five Degrees, and the Calculated Heats of Solution and Partial Molal Volumes II. *J. Biol. Chem.* **1935**, *109*, 231–248. [CrossRef]
36. Zhu, W.; Fan, Y.; Xu, Q.; Liu, X.; Heng, B.; Yang, W.; Hu, Y. Saturated solubility and thermodynamic evaluation of L-tryptophan in eight pure solvents and three groups of binary mixed solvents by the gravimetric method at T= 278.15–333.15 K. *J. Chem. Eng. Data* **2019**, *64*, 4154–4168. [CrossRef]
37. Batov, D.V.; Antonova, O.A.; Smirnova, N.L. Thermodynamics of the L-tryptophan interaction with glycerol or urea in water at ambient conditions. *J. Mol. Liq.* **2021**, *341*, 117352. [CrossRef]

38. Batov, D.V.; Kustov, A.V.; Smirnova, N.L. The temperature effect on the thermodynamics of the interaction of l-Tryptophan with urea and glycerol in water. *J. Therm. Anal. Calorim.* **2023**, *148*, 5521–5527. [CrossRef]
39. Görbitz, C.H.; Törnroos, K.W.; Day, G.M. Single-crystal investigation of L-tryptophan with Z´= 16. *Struct. Sci.* **2012**, *68*, 549–557. [CrossRef]
40. Rahal, O.; Hughes, C.E.; Williams, P.A.; Logsdail, A.J.; Diskin-Posner, Y.; Harris, K.D.M. Polymorphism of L-tryptophan. *Angew. Chem. Int. Ed.* **2019**, *58*, 18788–18792. [CrossRef]
41. Sosa-Rivadeneyra, M.; Zavala, A.; Rivas-Silva, J.F.; Uriza-Prias, D.; Bernès, S. Crystallization of the Third Polymorphic Modification of L-Tryptophan: A Case of Non-order–disorder Polytypism. *Cryst. Growth Des.* **2023**, *23*, 7031–7036. [CrossRef]
42. Ferreira, L.A.; Macedo, E.A.; Pinho, S.P. Solubility of amino acids and diglycine in aqueous–alkanol solutions. *Chem. Eng. Sci.* **2004**, *59*, 3117–3124. [CrossRef]
43. Cybulski, A.; Moulijn, J.A.; Sharma, M.M.; Sheldon, R.A. *Fine Chemicals Manufacture: Technology and Engineering*; Gulf Professional Publishing: Houston, TX. USA, 2001.
44. Kadam, S.S.; Kramer, H.J.; ter Horst, J.H. Combination of a single primary nucleation event and secondary nucleation in crystallization processes. *Cryst. Growth Des.* **2011**, *11*, 1271–1277. [CrossRef]
45. Kockmann, N.; Held, C.; Hohmann, L.; Hampel, R. Verfahren Zur Aufarbeitung Von L-Tryptophan. Germany Patent DE10 2018 100 810, 2018.

Disclaimer/Publisher's Note: The statements, opinions and data contained in all publications are solely those of the individual author(s) and contributor(s) and not of MDPI and/or the editor(s). MDPI and/or the editor(s) disclaim responsibility for any injury to people or property resulting from any ideas, methods, instructions or products referred to in the content.